Journal of Sciences, Islamic Republic of Iran 28(2): 133 - 146 (2017) http://jsciences.ut.ac.ir
University of Tehran, ISSN 1016-1104

Review Article

The Exploration Significance of Ag/Au, Au/Cu, Cu/Mo, (Ag×Au)/(Cu×Mo) Ratios, Supra-ore and Sub-ore Halos and Fluid Inclusions in Porphyry Deposits: A Review

H. Atapour*

Department of Mining Engineering, Faculty of Engineering, Shahid Bahonar University of Kerman, P.O.Box 76169-133, Kerman, Islamic Republic of Iran

Received: 13 April 2016 / Revised: 21 August 2016 / Accepted: 26 October 2016

Abstract

This paper documents the exploration significance of Ag/Au, Au/Cu, Cu/Mo and (Ag×Au)/Cu×Mo) ratios of the supra-ore and sub-ore halos versus fluid inclusion evolution for 24 Cu, 6 Cu- Mo and 10 Cu-Au porphyry deposits worldwide. The ratios are based only on the economic and mineralized hypogene alteration zones. The results indicate that (Ag×Au)/(Cu×Mo), Au/Cu and Cu/Mo ratios increase with decreasing depth and could be considered as the possible exploration guides for many as-yet-undiscovered unexposed porphyry deposits. These ratios are well correlated with vertical elemental vector zoning and alteration halos from the center (proximal potassic) outward (distal propylitic-zeolitic) and follow the order of Cu-Mo-Au, Cu-Zn, Zn-Pb-Ag, Ag-Pb- As-Sb-Hg-Au. On the basis of the (Ag×Au)/(Cu×Mo) ratios and fluid inclusion data, the Iranian continental arc porphyry copper deposits show multiphase halite-sylvite saturated fluid inclusions and formed between 2 to 4.75 km depth. The simple and multiple geochemical ratios and fluid inclusion evolution highlight that the Cu, Cu-Mo and Cu-Au porphyry deposits of the world were probably formed at <8-0.6, <5-2 and <4-1 km, respectively. This depth zoning could be used as an exploration target for hypogene as well as supergene mineralized zones, vectoring the position of ore body with respect to the primary halos or even level of erosion for unexposed porphyry systems. The main factors controlling the elemental ratios are related to the depth of mineralization, hydrothermal complexing of metal ligands and the presence or absence of sulfides minerals and gold-silver alloys.

Keywords: Geochemical ratios; Fluid inclusions; Depth of porphyry Cu; Cu-Mo; Cu-Au deposits.

Introduction

The exploration significance of Ag/Au, Au/Cu, Cu/Mo, and (Ag×Au)/(Cu×Mo) elemental ratios and fluid inclusion evolution in relation to depth of formation in porphyry and hydrothermal deposits is

* Corresponding author: Tel: +983432114041-9; Fax: +983432121003; Email: atapour@uk.ac.ir

poorly documented, though many porphyry systems show a centrally copper- rich proximal zone surrounded by Zn-Pb-Au-Ag distal aureole zone [1, 2, 3, 4, 5,6,7, 8, 9, 10, 11, 12, 13, 14, 15, 16, 17, 18, 19, 20, 21, 22, 23, 24, 25, 26, 27, 28, 29, 30, 31, 32, 33, 34, 35, 36, 37, 38, 39, 40, 41, 42, 43, 44, 45] .Experimental studies by Simon et al. [46], in the Cu-Fe-S system at 400 to 700°C indicate that most of the gold will be deposited in the high-temperature bornite-rich porphyry copper-gold deposits. Murakami et al. [47], reexamined valuable published data only on the Cu/Au ratios as an indication of formation depth of porphyry-style Cu-Au-Mo deposits, but their results have met with mixed success and overlapping of the similar Cu/Au ratios with different depths of porphyry ore formation, thus, the Cu/Au ratios gives some limitations. The main limitation is that copper could not display the role of a numerator, because its halos form before gold halos in the high temperature hydrothermal ores, thus the correct ratio should be presented as Au/Cu. According to Beus and Grigorian [48], the first prerequisite for the use of elemental ratios in hypogene hydrothermal depth zoning and supergene oxidation zone is related to the elements that form supra-ore halos in the low temperature shallow zones (e.g., Ag, Au) and sub-ore halos in the high temperature deeper zones (e.g., Cu, Mo). The standard elemental zoning proposed by Beus and Grigorian [48], follow vertically from the supra-ore halos (shallower) to the sub-ore halos (greater depth) as Ba-Sb-As-Hg-Cd-Ag-Pb-Zn-Cu-Bi-Mo-Co-Ni-U-Sn-Be-W. In this regard, vertical zonation of supra-ore and sub-ore halos could assess the position of the ore body with respect to the primary hypogene halos as well as the exposed level of erosion of geochemical anomalies [48].

The exploration use of Ag/Au, Au/Cu, Cu/Mo and (Ag×Au)/(Cu×Mo) has not been fully explored by the previous studies. The approaches in this paper are: (1) to assess the geochemical significance of the Ag/Au, Au/Cu, Cu/Mo ratios and a newly proposed (Ag×Au)/(Cu×Mo) ratio for exploration guides, and (2) present fluid inclusion data as a complementary possible exploration tool for the economic hypogene Cu, Cu-Mo and Cu-Au deposits worldwide.

Global distribution and tectonomagmatic aspects of porphyry deposits

Porphyry deposits form linear and narrow metallogenic provinces [49] with large, medium-to low grade deposits worldwide (Fig. 1) that are associated with Mesozoic to Cenozoic orogenic belts

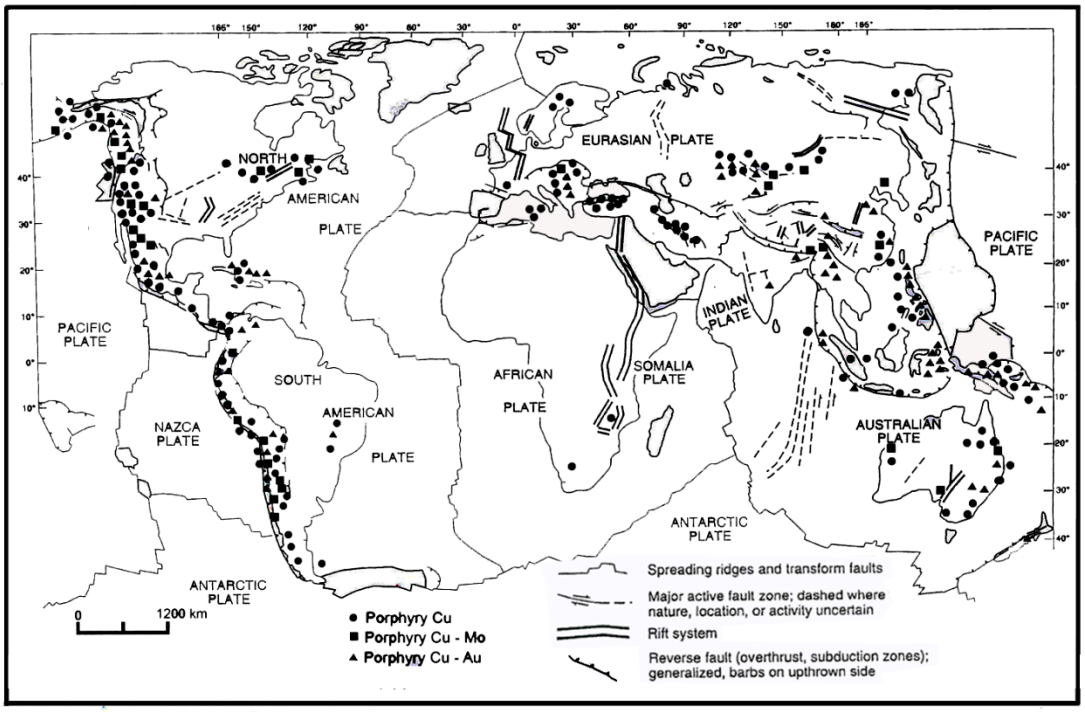

Figure 1. Approximate position of some Cu, Cu-Mo and Cu-Au porphyry deposits of the world (modified after [49, 50, 52, 53]).

Table 1. Tectonomagmatic and petrogeochemical aspects of some important porphyry deposits worldwide. (modified after [17, 49, 50, 52, 53]).

Porphyry deposits	Mo/Cu	SiO_2(%)	Productive intrusive rocks	Tectonic setting	Magmatic affinity	Potential byproducts	Exploration guides	Global examples
Cu (0.2-2 % Cu)	< 0.1	55-70	Diorite, granodiorite, quatz monzonite, tonalite and granite	Continental arc (flat –moderate subduction angles)	Calcalkaline, potassic calcalkaline and shoshonitic ± adakitic	Mo, Re, Au and Ag	Gossan, GIS, RS, IP, soil, mesquite and alluvial sampling	Sarcheshmeh (Iran) and El-Salvador (Chile)
Cu-Mo (0.2-1 % Cu)	0.1	55-70	Monzonite, quartz monzodiorite, monzogranite and granite	Continental arc	Calcalkaline, potassic calkalkaline and shoshonitic	Au and Ag	Gossan, RS, soil and alluvial sampling	Chuquicamata (Chile) and Bingham (America)
Cu-Au (0.1- 0.7 % Cu)	< 0.01	55-65	Diorite, syenite and monzodiorite	Island arc, post collisional arc ± continental arc	Potassic calcalkaline, shoshonitic and adakitic	Ag and PGE	Gossan, heavy minerals, soil and alluvial sampling for gold	Grasberg (Indonesia) and Kemes (Canada)
Mo (0.05- 0.5 % Mo)	>1	65-74 or > 74	Syenite, quatz monzonite, A-type granite and rhyolite	Anorogenic extensional rifting	Alkaline and calcalkaline	W and Sn	Aeromagnetic, and soil sampling for F and W	Climax and Mount Emmons (America)
Au (0.8- 2 ppm Au)	< 0.001	55-65	Diorite and syenite and quatz syenite	Island arc ± continental arc	Alkaline, shoshonitic and calcalkaline	Ag, Cu and Mo	Gossan, heavy minerals and soil sampling	Troilus (Canada) and Sulat (Philippines)

in western North and South America, around the western margin of the Pacific Rim, Europe, Central Asia, Middle East, major deposits in Paleozoic orogens of Central Asia and eastern North America and minor occurrences within Precambrian terrains [49, 50, 51, 52, 53]. They consist of composite stocks with typical porphyry textures and are formed in different tectonomagmatic settings, have diverse magmatic affinity and contain variable values of Cu, Mo, Au, Ag and potential byproducts (Table 1). Also, in Figure 2 some of the most important Iranian continental arc porphyry copper deposits are shown.

Materials and Methods

Importantly, the geochemical data on Ag/Au, Au/Cu, Cu/Mo, and (Ag×Au)/(Cu×Mo) ratios and bulk grade of economic porphyry deposits and or mines hosted by hypogene alteration zones are very limited worldwide (e.g.,[23, 47, 53, 54, 55]. In fact, precise and accurate Cu and Mo values in hypogene mineralized zones are reported for most of the economic porphyry deposits worldwide, but their Au, Ag and other metal contents, in particular formation depth and other factors could not be easily collected for this study by the author. This study excludes the geochemical data from the oxidation or supergene zones. Despite the limited geochemical data in this paper, important geochemical and fluid inclusion data on some of the Iranian porphyry copper deposits is presented [56, 57, 58, 59, 60]. However, some valuable geochemical data (e.g., [55, 60]) have been republished by Murakami et al. [47]; and Voudouris et al. [23]. In addition to these previously published data, new data are introduced on formation depth from some important Iranian continental arc porphyry copper deposits. The available existing geochemical data worldwide include about 24 Cu porphyry, 6 Cu-Mo porphyry and 10 Cu-Au (Table 2, 3 and 4) were selected from Canada (17), Iran (8), United State of America (6), Chile (6), Philippines (20), Kazakhestan (1), Argentina (1) and Armenia (1), respectively. Total tonnage, grades of Cu, Au, Mo and Ag and data on formation depth were compiled from the published compilations [17, 46, 47, 50, 53, 54, 55, 56, 57, 61, 62, 63, 64]. The main approach in this study is to compare the possible exploration significance of Ag/Au atomic mass, Au/Cu atomic mass × 10000, Cu/Mo atomic mass and (Ag×Au)/(Cu×Mo) atomic mass ratios in different types of porphyry deposits. The use of (Ag×Au)/(Cu×Mo) smooths out erratic analytical and sampling errors, thus allows a better

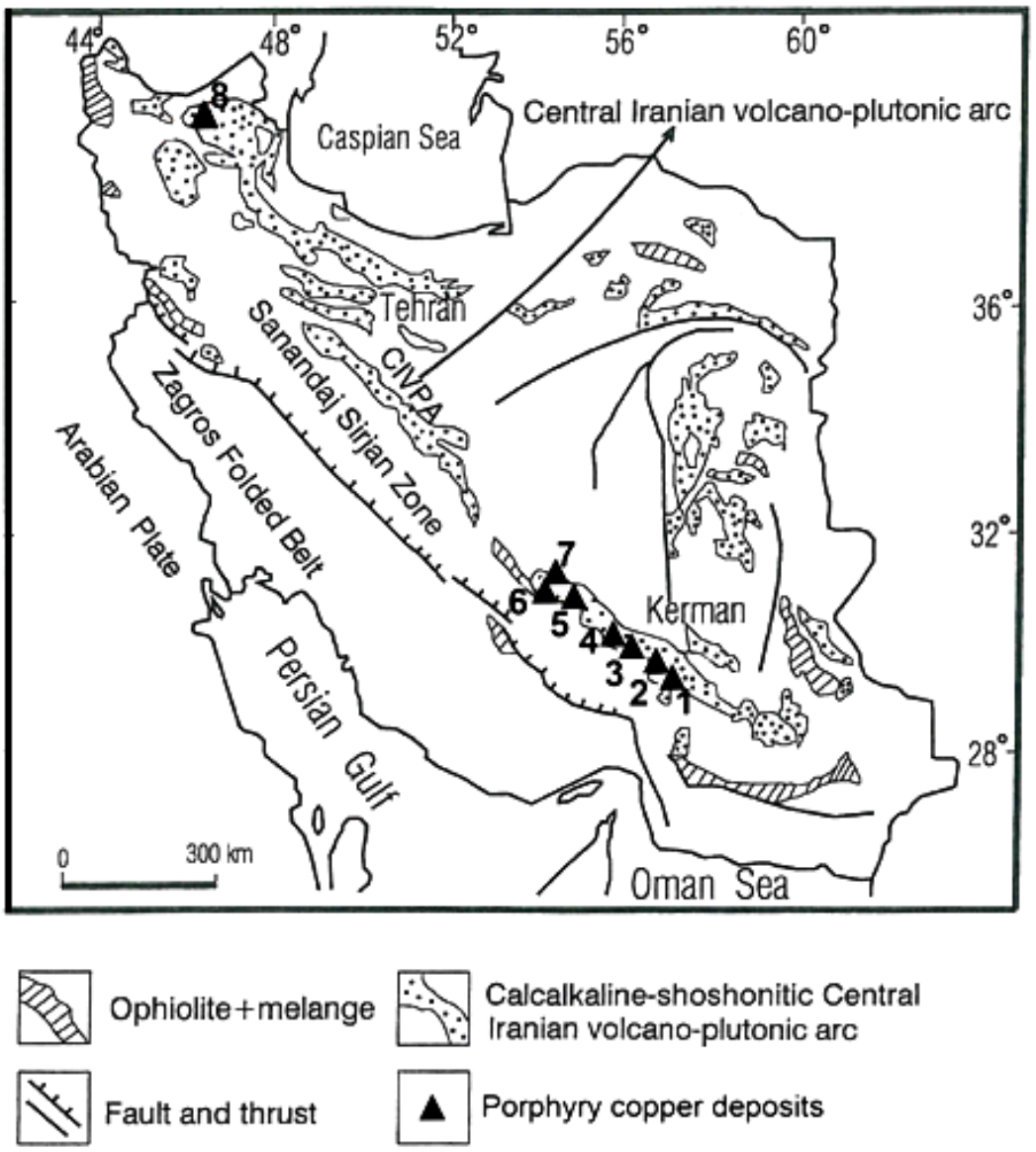

Figure 2. Geological map of Iran, showing the approximate position of some important continental arc porphyry copper deposits (modified after [50, 56, 57]). 1-Darrehamzeh, 2- Zaminhosien, 3- Darrehalu, 4- Sarcheshmeh, 5- Gode Kolvary, 6- Abdar, 7- Miduk, 8- Soungoun.

estimate of formation depth and exploration zoning than those of simple elemental ratios (Beus and Grigorian [48],).

Results and Discussion

The results of revised geochemical data on Ag/Au, Au/Cu×10000, Cu/Mo, and (Ag×Au)/(Cu×Mo) ratios are indicated in Table 2, 3 and 4 and also in Figure 3, 4 and 5 respectively. Accordingly, the highest Au/Cu, Cu/Mo and (Ag×Au)/(Cu×Mo) ratios are related to Cu porphyries and Cu-Au porphyry rather than Cu-Mo porphyry deposits. This might be related to the formation of immiscible sulfide liquids during crystallization of parent magma as has been reported by Simon et al. [46]. However, the highest Ag/Au ratios are developed in Cu and Cu-Mo porphyries.This is reflected to the lower gold contents in Cu-Mo porphyries [21]. According to Fig. 3, 4 and 5, the (Ag×Au)/(Cu×Mo) and Cu/Mo ratios increase with decreasing depth and vice versa in all types of porphyry deposits. The Ag/Au ratios increase with increasing depth in both Cu and Cu-Mo porphyries,

Table 2. Tonnage, grade, Ag/Au, Au/Cu× 10000, Cu/Mo and (Ag×Au)/(Cu×Mo) ratios in relation to formation depth of the selected Cu porphyry deposits.

Deposit (country)	Tonnage (Mt)	Cu (%)	Mo (%)	Ag (g/t)	Au (g/t)	Ag/Au	Au/Cu * 10000	Cu/Mo	Ag*Au/Cu*Mo	Formation depth (km)	Reference
Bethlehem (Canada)	677	0.45	0.016	0.4	0.005	80	111	28.00	0.28	3.9	1
Valley Copper (Canada)	800	0.48	0.01	1.9	0.006	316	125	48.00	2.38	4.8	1
Lornex (Canada)	514	0.43	0.015	1.2	0.006	200	139	28.00	1.12	4.4	1
Highmont (Canada)	265	0.27	0.041	0.9	0.004	225	148	7.00	0.33	3.9	1
Gibraltar (Canada)	965	0.32	0.01	0.9	0.07	12.85	2187	32.00	19.69	4.6	1
Granisle (Canada)	85	0.43	0.009	1.1	0.12	9.16	2790	48.00	34.11	1.2	1
Island Copper (Canada)	377	0.41	0.017	1.4	0.19	7.5	4634	24.00	38.16	1.5	1
Schaft Creek (Canada)	972	0.3	0.033	1.2	0.14	9	4667	9.00	16.97	0.6	1, 2
Morrison (Canada)	190	0.4	0.017	1	0.21	5	5250	24.00	30.88	1.2	1
Ann Mason (America)	495	0.4	0.01	0.001	0.01	0.1	250	40.00	0.03	3.3	3
Butte (America)	5220	0.67	0.028	8.6	0.042	204	627	24.00	19.25	7.5	3
Santa Rita (America)	3030	0.47	0.008	1.4	0.056	25	1191	59.00	20.85	6	3
Ely (America)	754	0.61	0.01	0.8	0.27	3	4427	61.00	35.41	3	4
El Salvador (Chile)	866	1.41	0.01	1.5	0.12	12.5	851	141.00	12.77	2	5
Agua Rica (Armenia)	1710	0.43	0.032	3.2	0.17	19	3953	14.00	39.53	2	6
Aktogai (Kazakhstan)	3200	0.39	0.008	1.1	0.029	38	744	49.00	10.22	2.1	7
Sarcheshmeh (Iran)	450	1.13	0.03	3.9	0.11	35	973	37.00	12.6	4.75	8, 9, 10
Miduk (Iran)	170	0.82	0.007	1.8	0.082	22	1000	117.00	25	2.51	9, 10, 11
Soungoun (Iran)	600	0.76	0.01	2.2	0.017	129	223	76.00	10	2	12
Abdar or Mosahim (Iran)	-	0.43	0.009	1.6	0.085	18	1976	47.00	35	2.85	9, 10
Gode Kolvary (Iran)	-	0.1	0.001	0.57	0.023	24	2300	100.00	131	2	9, 13
Darrehalu (Iran)	25	0.46	0.0065	1.44	0.034	42	739	70.00	16	2.1	9, 13
Zaminhosien or Babnam (Iran)	-	0.28	0.0003	0.98	0.07	14	2600	933.00	816	2.2	9
Darrehhamzeh (Iran)	-	0.1	0.0008	2.4	0.059	40	5900	12.50	1770	2.4	14

1: [47, 55], 2: [7, 47], 3: [6, 47], 4: [2, 47], 5: [47], 6: [1, 47], 7: [47], 8:[60], 9: [57], 10: [58], 11: [59], 12: [8], 13: [56], 14: [59].

probably indicating the presence of silver sulfosalts and electrum. In Cu-Au porphyries, the Ag/Au ratios increase with decreasing depth. There are no enough data on zoning aspects of the Ag/Au ratios in porphyry deposits. However, Einaudi [5]) reported a systematic increase of Ag/Au ratios toward the surface in Bingham porphyry copper mining district. The Au/Cu ratios in Cu porphyries increase from 111 to 5900 with

Table 3. Tonnage, grade, Ag/Au, Au/Cu×10000, Cu/Mo and (Ag×Au)/(Cu×Mo) ratios in relation to formation depth of the selected Cu-Mo porphyry deposits.

Deposit (country)	Tonnage (Mt)	Cu (%)	Mo (%)	Ag(g/t)	Au(g/t)	Ag/Au	Au/Cu*10000	Cu/Mo	Ag*Au/Cu*Mo	Formation depth (km)	Reference
Huckleberry (Canada)	161	0.48	0.015	0.93	0.025	156	521	32	3.23	2.3	1, 2
Brenda (Canada)	227	0.16	0.039	0.63	0.013	49	8125	4	1.31	4.4	1, 2
Berg (Canada)	250	0.4	0.03	5	0.05	100	1250	14	20.83	2	1, 2
Mineral Park (America)	172	0.46	0.032	2.2	0.027	82	587	15	4.04	4.4	3
Chuquicamata (Chile)	17100	0.65	0.04	5	0.013	384	200	16	2.50	4.5	4
Bingham (America)	3230	0.88	0.053	3.3	0.38	9	4318	17	30	2.5	3

1: [47 ,55], 2: [7], 3: [18, 47], 4: [10].

Table 4. Tonnage, grade, Ag/Au, Au/Cu×10000, Cu/Mo and (Ag×Au)/(Cu×Mo) ratios in relation to formation depth of the selected Cu-Au porphyry deposits.

Deposit (country)	Tonnage (Mt)	Cu (%)	Mo (%)	Ag(g/t)	Au (g/t)	Ag/Au	Au/Cu *10000	Cu/ Mo	Ag*Au/ Cu*Mo	Cu/Au *10000	Formation depth (km)	Reference
Laescondida (Chile)	4860	0.97	0.006	5	0.25	20	2577	161	214.78	38,800	3.2	3
Copper Mountain (Canada)	324	0.47	0.001	3.9	0.17	23	3617	470	1410.64	27647	1.1	1, 2
Bell (Canada)	495	0.36	0.005	1	0.16	6.25	4444	72	88.89	22,500	1.2	1,2
Tanama (eurto Rico)	126	0.64	0.005	1.7	0.38	5	8260	92	201.88	16842	3	4
Iron Max (Ajax) (Canada)	21	0.45	0.001	2	0.34	6	3445	450	1511.11	13,235	0.9	1, 2
Galore Creek (Canada)	316	0.68	0.001	7.9	0.52	32	3676	680	6041.18	13,077	1.2	1, 2
Kadzharan (Armenia)	181	0.65	0.05	2	0.65	3	10000	13	40.00	10,000	1.5	1, 2
Carribo Bell(Canada	293	0.23	0.001	4	0.3	14	13043	230	5217.39	7666	1	1, 2
Santo Tomas (philippines)	449	0.38	0.001	1.5	0.7	2	18421	380	2763.16	5,428	2	5

1:[47, 55], 2: [7], 3: [7, 14, 47], 3: [14], 4: [3], 5: [15].

decreasing depth. This is likely related to the ubiquitous presence of chalcopyrite at the greater depth of porphyry copper deposits [65]. Moreover, according to these authors, deep-seated porphyry copper-molybdenum deposits are deficient in gold values, contain higher modal contents of chalcopyrite and show lower Au/Cu ratios. At shallower depth, due to the presence of S and Au-rich vapor phase, the Au/Cu ratio will increase [65].

Cu/Mo ratios follow zoning patterns of sub-ore and supra-ore halos and depth zoning [48]. As such, the Cu/Mo ratios in in Cu, Cu/Mo and Cu-Au porphyries decrease with increasing depth. This indicates that molybdenite-rich porphyries are formed between 370-440 °C at greater depth and under low hydrostatic pressures [66].

In Cu-Au porphyry deposits (Table 4), the formation depth for majority of the deposits does not vary significantly (e.g., 0.9 to 1.2 km). However, Ag/Au, Cu/Mo and (Ag×Au)/(Cu×Mo) ratios increase with decreasing depth. This may be due to the higher values of Cu, Au and Ag and lower contents of Mo in

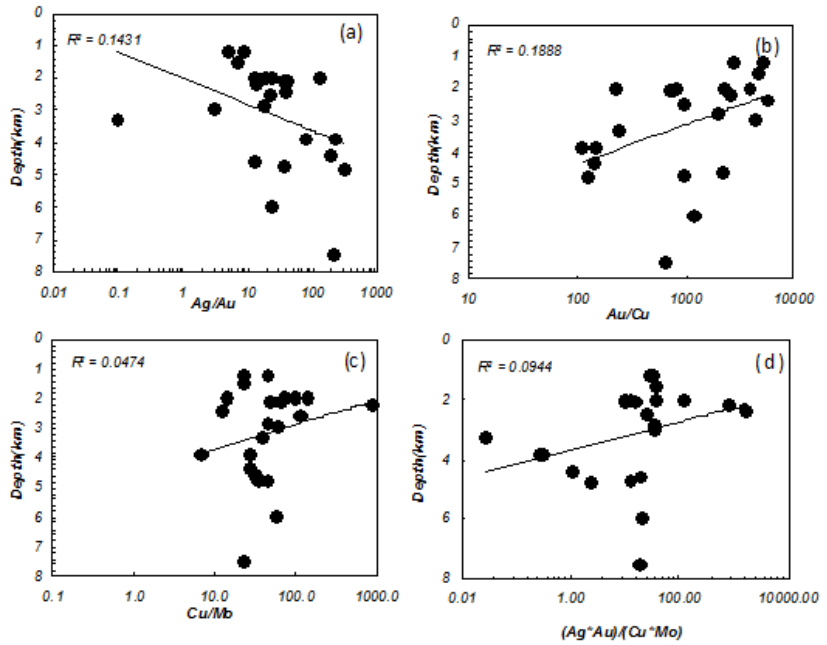

Figure 3 . Relationship between Ag/Au (a), Au/Cu (b), Cu/Mo (c) and Ag×Au/Cu×Mo (d) ratios and formation depth of the Cu porphyry deposits.

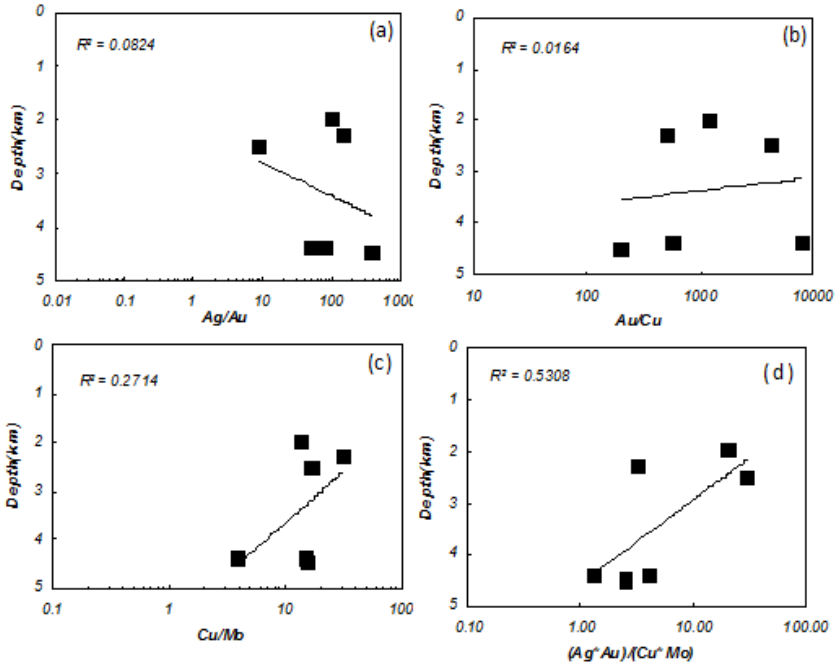

Figure 4. Relationship between Ag/Au (a), Au/Cu (b), Cu/Mo (c) and (Ag×Au)/(Cu×Mo) (d) ratios and formation depth of the Cu-Mo porphyry deposits.

Cu-Au porphyries. Au/Cu ratios do not show a well defined trend with depth.

In contrast to the simple Ag/Au, Au/Cu and Cu/Mo ratios, the use of multiplicative (Ag×Au)/(Cu×Mo) ratios give the best significant results, as the ratios for Cu, Cu-Mo and Cu-Au porphyry deposits increase with decreasing formation depth. This shows the potential role of Ag and Au supra-ore halos toward the surficial parts of the Cu, Cu-Mo and Cu-Au porphyries, thus could be considered as an exploration

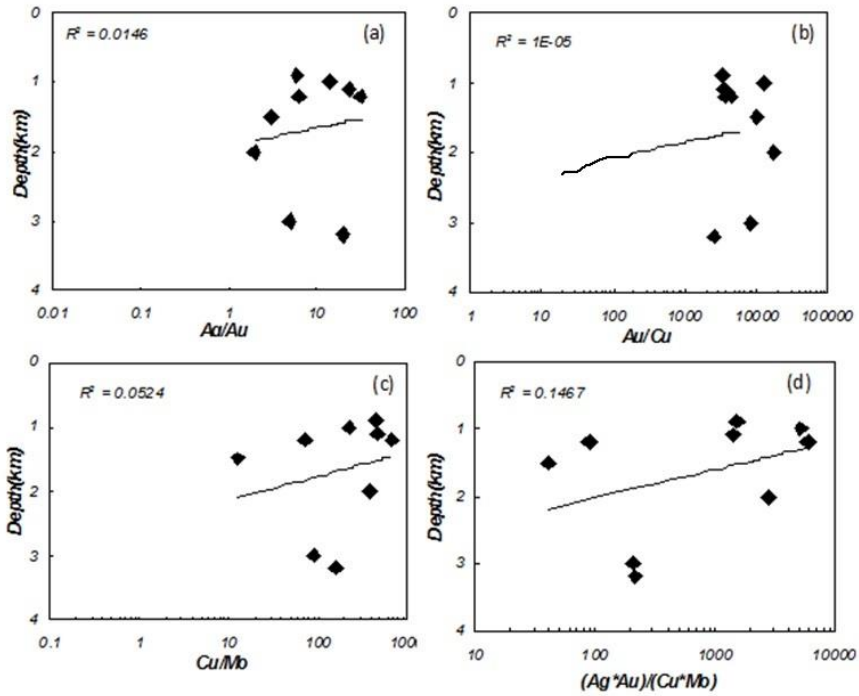

Figure 5. Relationship between Ag/Au (a), Au/Cu (b), Cu/Mo (c) and (Ag×Au)/(Cu×Mo) (d) ratios and formation depth of the Cu-Au porphyry deposits.

guide for prospecting unexposed porphyry deposits.

Beus and Grigorian [48] assume that for vertical zonation of supra-ore and sub-ore halos, the composition of hydrothermal fluids remains constant with time, but the depth of ore formation to be the main controlling factor. However, some minor factors could slightly influence the elemental ratios. These may include tectonic setting, lithology, pH-Eh and transporting ligands for metal complexes, respectively. Table 1 shows that continental arc Cu and Cu-Mo porphyries, postcollisional or Island arc Cu-Au porphyries and anorogenic Mo porphyries form in different tectonic settings. However, their Au/Cu, Cu/Mo and (Ag×Au)/(Cu×Mo) ratios (Fig. 3, 4 and 5) show the same increasing trend toward the surficial parts of the deposits. Although the chemical composition of productive intrusive rocks in terms of SiO_2 (Table 1) does not differ significantly, the Au/Cu, Cu/Mo and (Ag×Au)/(Cu×Mo) ratios display an increasing trend toward the shallower depth. In case that the composition of hydrothermal fluids changes with time [48], the zoning sequence may be controlled by hydrothermal transporting ligands. For example in most high temperature conditions (> 400 or 450 to 500 ºC) and acidic pH (4-5), high contents of Cu and Au are transported by chloride complexes of hypersaline fluids, which after cooling form considerable amounts of chalcopyrite-gold values in porphyry deposits [65]. This might influence the Au/Cu ratios, but there are no enough data to discuss this point. In contrast to this, below 400 °C, H_2S-rich solutions could transport and increase the solubility of gold to 1-10 ppm [65], but would not be able to transport considerable copper (< 1 ppm). Presumably, in this condition, the Au/Cu ratios will increase toward the low temperature zones or surficial part of the porphyry deposits. Also, the sulfide mineralogy could change the Au/Cu ratios in bornite or pyrrhotite-rich porphyry deposits [65]. Crystallization of pyrrhotite and bornite remove copper from the melt at a higher rate than it can remove gold, thus increasing the Au/Cu ratios [66]. The sequential deposition of molybdenite followed by chalcopyrite may change the Cu/Mo ratios in porphyry deposits. In this regard, molybdenite could precipitate before sericitic alteration in response to decreasing pH, but chalcopyrite is usually formed at lower temperatures during fluid neutralization [66]. This is consistent with the increasing trend of Cu/Mo ratios (Fig. 3, 4 and 5) toward the shallower depth in all porphyry deposits. Furthermore, the low Cu/Mo ratios in Mo-rich porphyry deposits are probably controlled by

Table 5. Geological, mineralogical, geochemical, tonnage grade, elemental ratios and estimated formation depth (fluid inclusion) of some important Miocene continental arc porphyry copper deposits, Iran.

Deposit	Volcanic rocks (Eocene)	Granitoid rocks (Miocene)	Hypogene Mineralization -alteration	Tonnage (Mt)	Cu (%)	Mo (%)	Ag (g/t)	Au (g/t)	Ag/ Au	Cu/ Mo	Au/Cu* 10000	Ag*Au /Cu*Mo	Formation depth (km)	Reference
Sarcheshmeh	Trachybasalt and trachyandesite	Quartz monzonite and granodiorite	Py, Cp, Mol, Sph, Po, Ga, Py/Cp= 12, Potassic-phyllic	450	1.13	0.03	3.9	0.11	35	37	973	12.6	4.75	1, 2
Miduk	Trachybasalt and basaltic andesite	Diorite and quartz diorite	Py, Cp, Mol, Py/Cu= 3-12 Potassic-phyllic	170	0.82	0.007	1.8	0.082	22	117	1000	25	2.51	3, 4
Soungoun	Dacite and trachyandesite	Monzonite and quatrtz monzonite	Py, Cp, Mo, Py/Cp = 2-12 Potassic-phyllic	600	0.76	0.01	2.2	0.017	129	76	223	10	2	3, 5
Abdar (Mosahim)	Dacite and trachyandesite	Diorite and quartz diorite	Py, Cp, Ga, Sph, Mol, Py/Cp = 16, Potassic-phyllic	-	0.43	0.009	1.6	0.085	18	47	1976	35	2.85	1, 3
Gode- Kolvari	Trachybasalt and trachyandesite	Diorite and quartz diorite	Py, Cp, Mol, Py/Cp = 12 Potassic-phyllic	-	0.1	0.001	0.57	0.023	24	100	2300	131	2	6, 7

1:[58], 2: [60], 3: [59], 4: [59], 5: [8], 6:[50], 7: [57]. 8: [51]. Py= pyrite, Cp= chalcopyrite, Mol= molybdenite, Ga= galena and Sph= sphalerite and Po= pyrrhotite.

thiomolybdate-sodium complexes, low chlorine concentrations and high fugacity of H_2O [66].

Fluid inclusion evolution versus elemental ratios and formation depth.

According to Bodnar [67], pressure release via lithostatic to hydrostatic transition causes the fluid phase separation into brine and vapour phases. This will result in a wide range in the fluid inclusion salinities (0 - 70 wt % NaCl equivalent), homogenization temperatures (200 - 700 ºC) and formation depth (1-7km) for different porphyry deposits. Geological, mineralogical, geochemical, elemental ratios and formation depth of some important Iranian continental arc porphyry copper deposits are shown in Table 5. The most distinguishing feature of the fluid inclusion data in some of the Iranian porphyry copper deposits, is the common occurrence of highly saline inclusions scheme of Bodnar [67], containing multiple daughter minerals including halite, sylvite, hematite and chalcopyrite. Figure 6a illustrates an example of multiphase halite – saturated fluid inclusion in Gode Kolvary Miocene porphyry copper deposit. These types of fluid inclusions coexist with low density vapor phase, thus have been formed by the liquid-vapor phase separation of an intrinsic part of the magmatic-hydrothermal evolution.

The common occurrence of halite and hematite as daughter minerals of magmatic-related inclusions (Fig. 6b) indicates the high level of dissolved Fe and considerable high oxygen fugacity in such fluids, thus Fe is a major component of such solutions, together with Na and K similar to those reported by Bodnar [67]. The interpretation of fluid inclusion data from Gode Kolvary porphyry copper deposit in Iran is shown in Table 5, Fig. 6c and 6d and by the use of P-X and P-T phase diagram in NaCl-H_2O system (Fig. 7). The highest homogenization temperature was found to be around 600 ºC with salinity of about 70 wt % NaCl equivalent (Fig. 6d), corresponding to potassic alteration. Furthermore, the presence of chalcopyrite crystals in fluid inclusions supports the granitoid related fluids of magmatic origin, in particular of potassic-phyllic alteration zone. According to the geological reconstruction of the area [50, 63], the total estimated stratigraphic thickness of the overlying rocks at the time of porphyry intrusive emplacement at Gode Kolvari porphyry system is estimated to have been about 2 km, which corresponds to a lithostatic pressure of about 500 bars or a hydrostatic pressure of 200 bars. Therefore, the maximum formation depth of the Miocene Gode Kolvary porphyry copper deposit is about 2 km. The exploration significance of formation depth in continental arc porphyry copper deposits of Iran is indicated in Table 5. The Sarcheshmeh deposit has been reported to have been formed at 4.75 km depth [58, 60].

Possible exploration model

The relationship between elemental ratios with

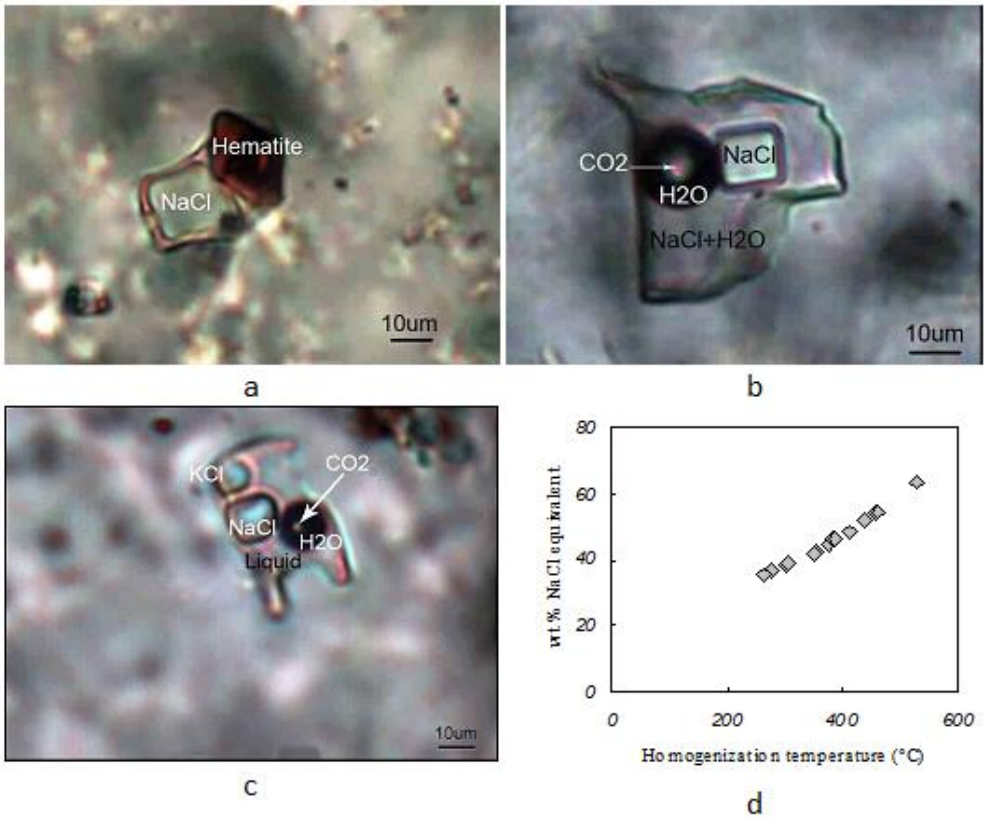

Figure 6. Photomicrograph illustrating a) hematite-rich multiphase aqueous, b) a primary polyphase halite-saturated, c) polyphase halite and sylvite saturated aqueous fluid inclusions from the Miocene Gode Kolvary porphyry copper deposit, Iran and d) salinity versus homogenization temperature of the fluid inclusions from the some important Miocene continental arc porphyry copper deposits, Iran.

formation depth and their regional or detail exploration potential in porphyry deposits has not been fully explored in the literatures. In this paper, we discuss the exploration significance of the Ag/Au, Au/Cu, Cu/Mo and (Ag×Au)/(Cu×Mo) ratios in three different types of porphyry deposits.

In Cu, Cu-Mo and Cu-Au porphyry deposits, the Au/Cu, Cu/Mo and (Ag×Au)/(Cu×Mo) ratios display an increasing trend with decreasing depth. This indicates the presence of the argentite, silver bearing sulfosalts, electrum and gold in the shallowest part of the porphyry deposits, probably in the phyllic, propylitic and advanced argillic ore zone. It also indicates that most of the Cu and Mo ores is formed in the deepest zone of potassic-sericitic alteration as suggested by Chaffee [68]. The higher Au/Cu ratios may reflect that the gold grade increases toward surface, indicating the role of S-rich bisulfide complexes below 300° C and enrichment of gold at low-temperature zones [55, 65].

The Ag/Au ratios in selected porphyry Cu and Cu-Mo deposits increase with increasing depth. This is possibly related to the role of silver chloride complexes at higher temperatures, which after cooling formed argentite, tetrahedrite, , native silver and electrum in potassic-sericitic zone of porphyry deposits. In this regard, Chaffee [68] reported strong anomaly for silver in potassic-sericitic zone of the Kalamazo porphyry deposit. The Ag/Au ratios in selected Cu-Au porphyry deposits increase with decreasing depth, which may be related to the predominant occurrences of acanthite and electrum toward the shallowest zone of the propylitic and advanced argillic alteration. This is consistent with the Ag/Au ratios and metal zoning around Bingham porphyry systems, as reported by Einaudi [5]. Interestingly enough, Chaffee [68], found high values of silver in the propylitic alteration zone, surrounding the Kalamazo porphyry deposit. Thus, the use of Ag/Au ratios in propylitic alteration zone is the most

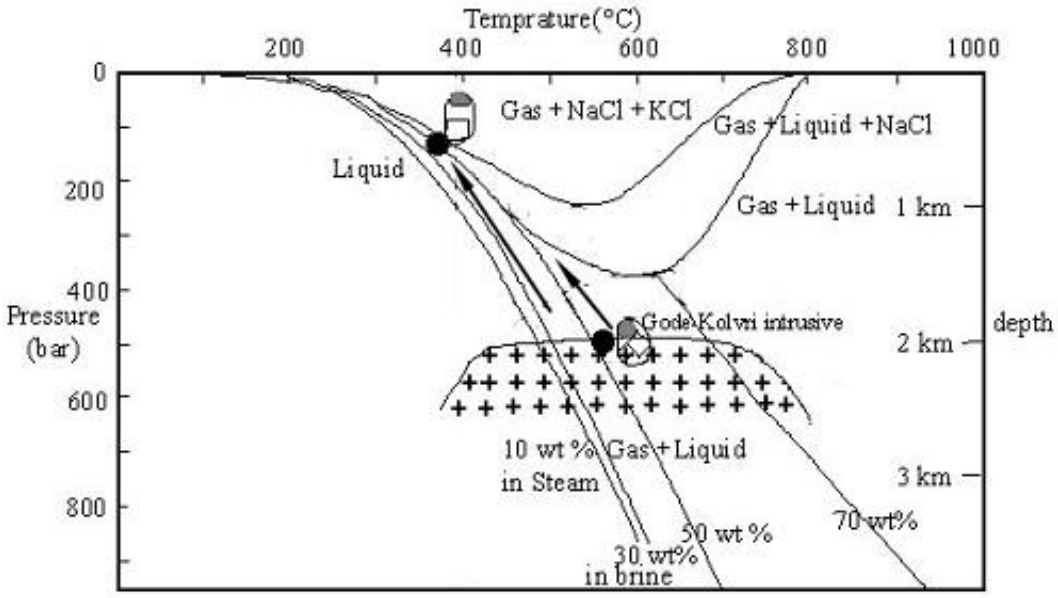

Figure 7. P-T diagram (Brathwaite et al. [50, 63, 69], relevant to interpretation of microthermometric of the polyphase fluid inclusion data from the Miocene Gode Kolvary porphyry copper deposit, Iran.

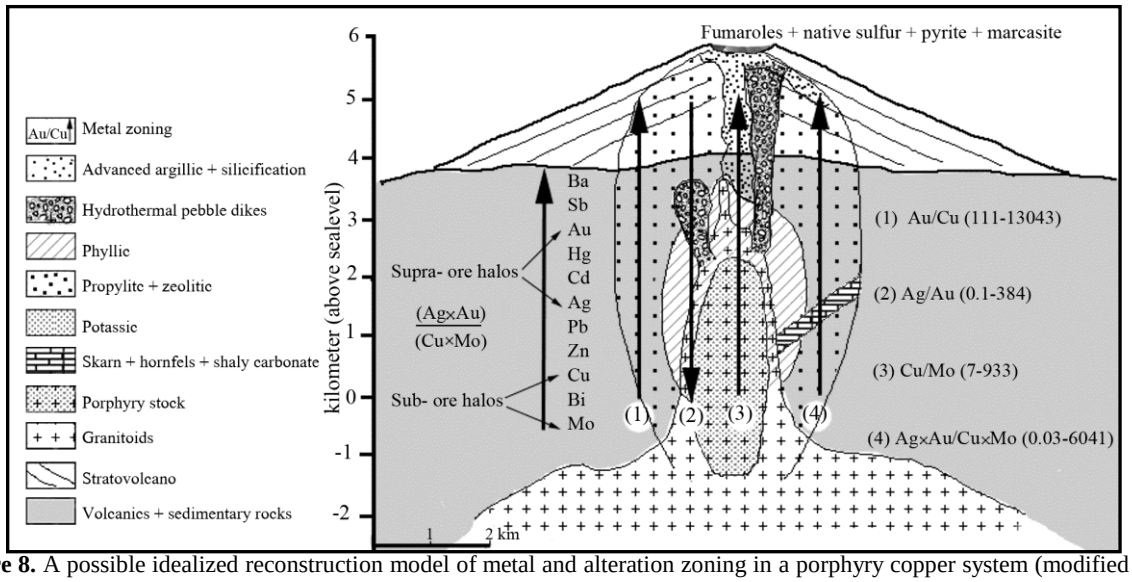

Figure 8. A possible idealized reconstruction model of metal and alteration zoning in a porphyry copper system (modified after [17, 21, 48, 65]). The vectors indicate increasing or decreasing trend of elemental ratios. The variations for each elemental ratios are shown in parentheses versus formation depth of porphyry deposits (111-13043). The sequences of supra-ore and sub-ore elemental halos are shown in the left side of the figure.

suitable exploration guide for estimating the vein-type silver-gold mineralization and the proximity to the underlying potassic-phyllic ore zone. The relationship between (Ag×Au)/(Cu×Mo) ratios and formation depth is significantly better developed in all types of porphyry deposits, as the ratios are meaningfully increased with decreasing depth. Therefore, it is expected that the main Cu-Mo ore body exists at greater depth. This relation is compatible with the suggestions of Beus and Grigorian [48] that higher gold and silver values develop toward the shallowest and at low-temperature zone of porphyry-hydrothermal deposits.

Although alteration and zoning model of porphyry mineralization have been proposed by Sillitoe [21] and Kouzmanov and Pokrovoski [65], no model of supra-

ore or sub-ore elemental ratios has yet been suggested. To modelize the elemental ratios, an idealized reconstruction model of porphyry system is revised in Fig. 8. Accordingly, the variations on the (Ag×Au)/(Cu×Mo), Au/Cu, Cu/Mo and Ag/Au ratios are depicted by vector zoning. This is consistent with the order of elemental halos and alteration zoning of Beus and Grigorian [48]. The illustration shows that the Ag/Au ratios increase toward the deepest zone of the ore body, whereas the Au/Cu, Cu/Mo—and (Ag×Au)/(Cu×Mo) ratios give an increasing trend toward the surficial part of the porphyry deposit. This increasing trend demonstrates that the main Cu, Cu-Mo and even Cu-Au porphyries exist below the supra-ore halos and in the deeper part of the mineralized zone.

Conclusion

This investigation highlights that the anomalous supra-ore and sub-ore halos have the potential to assess the relative position of the main porphyry ore zone with respect to the primary hydrothermal halos at different depths or to indicate the exposed level of the mineralized zones.

The increasing trend of Au/Cu ratios toward the surficial parts of all porphyry deposits might be related to low temperature fluids, bisulfide gold complexes and the presence of bornite or pyrrhotite-rich porphyry and epithermal systems.

The main controlling factors for Cu/Mo ratios in all porphyry deposits include depth of formation, specific thiomolybdate-sodium complexes, low temperature of hydrothermal fluids, the low concentration of chloride complexes and the high fugacity of H_2O.

The (Ag×Au)/(Cu×Mo) ratios reflect a better response to formation depth, hydrothermal zoning and alteration halos than the other elemental ratios and may be used as an exploration guide for all genetic types of the porphyry deposits.

Based on the (Ag×Au)/(Cu×Mo) ratio, the Cu, Cu-Mo and Cu-Au porphyry deposits formed at <8-0.6 km, < 5-2 km and <4-1 km, respectively.

We suggest that the use of (Ag×Au)/(Cu×Mo) ratios in drill core samples of any porphyry systems may guide to determine the depth of the main Cu-Mo-Au mineralized zone or to evaluate the exposed level of many as-yet-undiscovered unexposed porphyry deposits.

Although, the anomalous supra-ore and sub-ore halos in this investigation were developed in hypogene mineralized zones, they are also useful in providing the exploration insights into gossan zones that cap the underlying sulfide enrichment and hypogene zones of the unexposed porphyry deposits.

Acknowledgements

I am grateful to Prof. Dr. M R. Nooridaloii, Editor-In-Chief of Journal of Sciences of Islamic Republic of Iran, the Editorial Board and the anonymous reviewers for their professional editorship, regarding the reviewing processes of the manuscript. Also, I appreciate the authors of the several papers, which I have benefited from their knowledge for this paper. I would like to thank the encouraging support of my colleagues at Geological Survey of Kerman, Department of Mining Engineering and Department of Geology of Shahid Bahonar University of Kerman, Kerman, Iran.

References

1. Koukharsky M., and Mirre J. C., Vida prospect: a porphyry copper - type deposit in northwestern Argentina. *Econ. Geol.* **102**: 849-863 (1976).
2. Roedder E., Natural occurrence and significance of fluids indicating high pressure and temperature. *Phys. Chem. Earth.* **13**: 9-39 (1981).
3. Cox D. P., Geology of the Tanama and Helecho porphyry copper deposits and their vicinity. *US. Geol. Surv*. 95p. (1985).
4. Catchpole H., Kouzmanov K., Putlitz B., Seo J. H., and Fontboté L. Zoned base metal mineralization in a porphyry system: origin and evolution of mineralizing fluids in the MorocochadDistrict, Peru. *Econ. Geol*. **110**: 39-72 (2015).
5. Einaudi M. T. Ag/Au ratios in time and space in the Bingham Mining District, Utah: Implications for genesis and exploration. *Soc. Econ. Geol. Internat. Exch. Lect*. 5p. (1994).
6. Dilles J.H. and Proffett J.M. Metallogenesis of the Yerington batholith, Nevada. In: Pierce FW Bolm JG (Eds.), Porphyry copper deposits of the Cordillera, Tucson. *Arizona. Geol. Soc. Digest*. **20**: 306-315 (1995).
7. Schroeter T. G. Porphyry deposits of the north western Cordillera of North America. *Can. Ins. Min. Metal. Petrol*. **46** (1995).
8. Hezarkhani A. and Williams-Jones A. E. Controls of alteration and mineralization in the Soungoun porphyry copper deposit, Iran: Evidence from fluid inclusions and stable isotopes. *Econ. Geol.* **93**: 651-670 (1998).
9. Seo J. H., Guillong M., Heinrich Ch. A. Separation of Molybdenum and Copper in Porphyry Deposits: The Roles of Sulfur, Redox, and pH in Ore Mineral Deposition at Bingham Canyon. *Econ. Geol.* **107**: 333-325 (2012).
10. Ossandon G.C., Freraut R.C., Gustafson L.B., Lindsay D.D. and Zentilli M. Geology of the Chuquicamata Mine: a progress report. *Econ. Geol.* **96**: 249-270 (2001).
11. Hou Z., Pan X., Li Q., Yang Z. and Song Y. The giant Dexing porphyry Cu–Mo–Au deposit in east China: product of melting of juvenile lower crust in an

intracontinental setting. *Mineral. Deposita* **48**: 1019–1045 (2013).
12. Jowitt S. M., Mudd G. M., Weng Z. Hidden mineral deposits in cu-dominated porphyry-skarn systems: how resource reporting can occlude important mineralization types within mining camps, *Econ. Geol.* **108**: 1185-1194 (2013).
13. Landtwing M.R., Furrer C., Redmond P.B., Pettke T., Guillong M. and Heinrich Ch. A. The Bingham Canyon Porphyry Cu-Mo-Au Deposit. Zoned Copper-Gold Ore Deposition by Magmatic Vapor Expansion. *Econ. Geol*. **107**; 91 – 118 (2010).
14. Padilla-Garza R.A., Titley S.R. and Eastoe C.J. Hypogene evolution of the Escondida porphyry copper deposit, Chile. *Econ. Geol. Spec. Publ.* **11**: 141-165 (2004).
15. Imai A. Generation and evolution of ore fluids for porphyry Cu-Au mineralization of the Santo Tomas II (Philex) deposit, Philippines. *Res. Geol.* **55**: 73-90 (2001).
16. Cooke D.R., Hollings P., Wilkinson J.J. and Tosdal R.M. Geochemistry of porphyry deposits. In: Holland H. and. Turekian K. (Eds.) *Treatise on Geochemistry*, 2nd Ed., pp. 357- 376 (2014).
17. Berger B.R., Ayuso R.A., Wynn J. C. and Seal R.R. Preliminary model of porphyry copper deposits. *US. Geol. Surv*. 55 p. (2008).
18. Rusk B.G., Reed M.H. and Dilles J.H. Fluid inclusion evidence for magmatic-hydrothermal fluid evolution in the porphyry copper-molybdenum deposit at Butte, Montana. *Econ. Geol.* **103**: 307-334 (2008).
19. Imai A., Suerte, L.O., and Nishihara S. Origin of bornite pods in intrusive rocks at the Kingking porphyry copper-gold deposits, Southeastern Minadanao, Philippines. *Res. Geol.* **59**: 307-313 (2009).
20. Imai A., and Nagai Y. Fluid inclusion study and opaque mineral assemblages at the deep and shallow part of the Batu Hijau porphyry copper-gold deposit, Sumbawa, Indonesia. *Res. Geol.* **59**: 231-243 (2009).
21. Sillitoe R.H. Porphyry copper systems. *Econ. Geol.* **105**: 3-41(2010).
22. Aftabi A., and Atapour H. Alteration geochemistry of volcanic rocks around Sarcheshmeh porphyry copper deposit, Rafsanjan, Kerman, Iran: Implications for regional exploration. *Res. Geol.* **61**: 76-90 (2011).
23. Voudouris P., Melfos V., Spry P.G., Bindi L., Moritz R., Ortelli M. and Kartal, T. Extremely Re-Rich Molybdenite from Porphyry Cu-Mo-Au Prospects in Northeastern Greece: Mode of Occurrence, Causes of Enrichment, and Implications for Gold Exploration. *Minerals*, **3**: 165-191(2013).
24. Watanabe S., and Hayashi K. Mineralogy, sulfur isotopes and fluid inclusion studies of hydrothermal ore at the Khakurei deposit, Bayonnaise Knoll, Izu-Bonin arc. *Res. Geol.* **64**: 77-90 (2014).
25. Sun W. , Huang R., Li H., Hua Y., Zhang Ch., Sun S., Zhang L., Ding X., Li C., Zartmana R.E., and Ling M. Porphyry deposits and oxidized magmas, *Ore. Geol. Rev.* **65** 97–131 (2015).
26. Liang H.Y., Sun W.D., Su W.C., and Zartman R.E. Porphyry copper–gold mineralization at Yulong, China promoted by decreasing redox potential during magnetite alteration. *Econ. Geol*. **104**: 587–596 (2009).
27. Shafiei B., Haschke M., Shahabpour J. Recycling of orogenic arc crust triggers porphyry Cu mineralization in Kerman Cenozoic arc rocks, southeastern Iran. *Mineral. Deposita* **44**: 265–283 (2009).
28. Shen P., Shen Y.C., Pan H.D., Wang J.B., Zhang R., and Zhang Y.X. Baogutu porphyry Cu–Mo–Au deposit, West Junggar, northwest China: petrology, alteration, andmineralization. *Econ. Geol*. **105**: 947–970 (2010).
29. Wilkinson J.J. Triggers for the formation of porphyry ore deposits in magmatic arcs. *Geosciences*. **6**: 917–925 (2013).
30. Liu L., Richards J.P., Creaser R.A., DuFrane S.A., Muehlenbachs K., and Larson P.B. Geology and age of the Morrison porphyry Cu–Au–Mo deposit, Babine Lake area, British Columbia. *Can. J. Earth. Sci*. **53**: 950-978 (2016).
31. Hou Z., Zhang H., Pan X., and Yang Z. Porphyry Cu (–Mo–Au) deposits related to melting of thickened mafic lower crust: examples from the eastern Tethyan metallogenic domain, *Ore. Geol. Rev.* **39**: 21–45 (2011).
32. Shafiei B., and Shahabpour J., Geochemical aspects of molybdenum and precious metals distribution in the Sarcheshmeh porphyry copper deposit, Iran. *Mineral. Deposita* **47**: 535-543 (2012).
33. Corbett G. Anatomy of porphyry-related Au-Cu-Ag-Mo mineralised systems: Some exploration implications. *AIG Bull.* **49**: 33-46 (2009).
34. Mao J., Zhang J., Pirajno F., Ishiyama D., Su H., Guo C., and Chen Y. Porphyry Cu–Au–Mo–epithermal Ag–Pb–Zn–distal hydrothermal Au deposits in the Dexing area, Jiangxi province, East China, A linked ore system. *Ore Geol. Rev*. **43**: 203–216 (2011).
35. Volkov, A., Serafimovski, T., Tasev, G. Porphyry Cu-Mo-Au-Ag-deposits of the northeast of Russia, comparison with similar deposits of the R. Macedonia segment of the Tethys belt. *Geol. Macedonica*, **3**: 73-82 (2012).
36. Eliopoulos D.G., Economou-Eliopoulos M., and Zelyaskova-Panayiotova M. Critical factors controlling Pd and Pt potential in porphyry Cu–Au deposits: evidence from the Balkan Peninsula. *Geosciences* **4***:* 31-49 (2012).
37. Rabbia O.M., Hernández L.B., French D.H., King R.W., and Ayers J.C. The El Teniente porphyry Cu–Mo deposit from a hydrothermal rutile perspective. *Mineral. Deposita*, **44**: 849-866 (2009).
38. Gruen G., Heinrich Ch.A., and Schroeder K. The Bingham Canyon porphyry Cu-Mo-Au deposit. II. vein geometry and ore shell formation by pressure-driven rock extension. *Econ. Geol*. **105**:69-90 (2013).
39. Porter T.M. The geology, structure and mineralisation of the Oyu Tolgoi porphyry copper-gold-molybdenum deposits, Mongolia: A review. *Geosci. Fron*. **7**: 375–407 (2016).
40. Redmond P.B. and Einaudi M.T. The Bingham Canyon porphyry Cu-Mo-Au deposit. I. sequence of Intrusions, vein formation, and sulfide deposition. *Econ. Geol*. **105**: 43-68 (2010).
41. Kyser T.K., Clark A.H., Stanley C.R., and Oates Ch.J. Lithogeochemistry of the Collahuasi porphyry Cu–Mo and epithermal Cu–Ag (–Au) cluster, northern Chile: Pearce element ratio vectors to ore Esteban Urqueta. *Geochem. Explor. Environ. Anal*. **9**: 9–17 (2009).

42. Fox N., Cooke D.R., Harris A.C., Collett D. Eastwood G. Porphyry Au-Cu mineralization controlled by reactivation of an arc - transverse volcano-sedimentary subbasin. *Geology* **43**: 811-814 (2015).
43. Djouka-Fonkwé M.L., Kyser K., Clark A.H. Urqueta E., Oates Ch.J., and Ihlenfeld Ch. Recognizing propylitic alteration associated with porphyry Cu-Mo deposits in lower greenschist facies metamorphic terrain of the Collahuasi district, northern Chile—implications of petrographic and carbon isotope relationships. *Econ. Geol*. **107**: 1457–1478 (2012).
44. Shen Ch.P., Shen, Y., Liu T., Meng L., Dai H., and Yang Y. Geochemical signature of porphyries in the Baogutu porphyry copper belt, western Junggar. *Gondwana Res*. **16**: 227–242 (2009).
45. Kelley K.D., Lang J., Eppinger R.G. Exploration geochemistry at the giant pebble porphyry Cu–Au–Mo deposit, Alaska. *SEG News* **80** 1–23 (2010).
46. Simon G., Kesler S.E., Essene E.J. and Chryssoulis S.L. Gold in porphyry copper deposits: experimental determination of the distribution of gold in the Cu-Fe-S system at 400℃ to 700℃. *Econ. Geol*. **95**: 259-270 (2000).
47. Murakami H., Seo J.H., and Heinrich C.A. The relation between Cu/Au ratio and formation depth of porphyry-style Cu-Au-Mo deposits. *Mineral. Deposita* **5**: 11-21 (2010).
48. Beus A.A., and Grigorian S. *Geochemical exploration methos for mineral deposits*. Applied Publishing Co., Wilmette, Illinois, 287p. (1977).
49. Pirajno F. *Hydrothermal processes and mineral systems*, Springer, 1250 p. (2009).
50. Atapour H. Geochemical evolution and metallogeny of potassic igneous rocks of Dehaj-Sarduieh volcano-plutonic belt, Kerman province with particular refertence to special elements, Unpublished Ph.*D Thesis*, Shahid Bahonar University of Kerman, Iran, 401 p. (In Farsi with English abstract) (2007).
51. Mehrpartou M. Contribution to the geology, geochemistry, ore genesis and fluid inclusion investigations on Sungun Cu–Mo porphyry deposit, *Ph.D. Thesis* University of Hamburg, 245 p. (1993).
52. Sinclair W.D. Porphyry deposits. In: Goodfellow W.D. (Eds.), *Mineral deposits of Canada*. Geological Association of Canada, Special publication, **5**: pp. 223-243 (2007).
53. Singer D.A., Berger V., and Moring B.C. Porphyry copper deposits of the world: database and grade and tonnage models. *US. Geol. Surv.* 1155 p. (2008).
54. Cox D.P., and Singer D.A. Distribution of gold in copper deposits. *US. Geol. Surv.* 88-46 (1988).
55. Sutherland Brown A. Porphyry deposits of the Canadian Cordillera of Norh America. *Can. Inst. Min. Metal. Petrol*. 510 p. (1976).
56. Aftabi A. Geochemical aspects of sheared zones as an indication of porphyry Cu-Mo-Au-Ag mineralization at Derehamzeh, Jiroft, Kerman, Iran. *Explor. Min. Geol.* **l6**: 261-267 (1997).
57. Atapour H., and Aftabi, A. The geochemistry of gossans associated with Sarcheshmeh porphyry copper deposit, Rafsanjan, Kerman. Iran: Implications for exploration and the environment. *J. Geochem. Explor.* **93**: 47-65 (2007).
58. McInnes B.I.A., Evans N.J., Fu F.Q., and Garwin S. Application of thermochronology to hydrothermal ore deposits. *Reviews in Mineralogy and Geochemistry.* **58**: 517-520 (2005).
59. Taghipour N. and Aftabi A. Fluid inclusion microthermometry at the Miduk porphyry copper deposit, Kerman, Iran. *In Proceedings Goldschmidt Conference Abstracts*, A1304 (2009).
60. Waterman G.C. and Hamilton R.L. The Sarchesmeh porphyry copper deposit. *Econ. Geol.* **70**: 568-576 (1975).
61. Aftabi A. and Atapour H. Comments on "Arc magmatism and subduction history beneath the Zagros Mountains, Iran: A new report of adakites and geodynamic-consequences"by J. Omrani, P. Agard, H. Whitechurch, M. Bennoit, G. Prouteau, L. Jolivet, *Lithos* **113** 844–846 (2009).
62. Aftabi A., and Atapour H. Regional aspects of shoshonitic volcanism in Iran. *Episodes* **23:**119-125 (2000).
63. Atapour H., and Aftabi H. Geochemistry and metallogeny of calckalkaline, shoshonitic and adakitic igneous rocks associated with Cu- Mo vein type deposits of Dehaj-Sarduieh volcanio- plutonic belt, Kerman. *J. Geosciences*, **72**: 161-172 (In Persian with English abstract), (2009).
64. Atapour H., and Aftabi H. Geochemical characteristic of tourmaline as a prospecting guide for porphyry orebodies and granitoid rocks in Kerman province, *J. Geosciences*, **40-41**:38- 59 (In Persian with English abstract), (2002).
65. Kouzmanov K. and Pokrovski G.S. Hydrothermal controls on metal distribution in porphyry Cu (Mo-Au) systems. *Soc. Econ. Geol. Inc. Special Publ.* **16**: 573-618 (2012).
66. Spencer E. T. The transport and deposition of molybdenum in porphyry ore system, *Unpublished Ph.D Thesis*, Imperial College of London, 318 p. (2015).
67. Bodnar R.J. Fluid inclusion evidence for a magmatic source for metals in porphyry copper deposits. In: Thompson J.F.H. (Eds.), *Magmas, fluids and ore deposits*, Mineralogical Association of Canada, Short Course , **23**:139-152 (1995).
68. Chaffee M. A. The zonal distribution of selected elements above the Kalamazoo porphyry copper deposit, San Manuel District, Pinal County, Arizona. *J. Geochem. Explor.* **5**: 145-165 (1976).
69. Brathwaite R.L., Simpson M.P., Faure K., and Skinner D.N.B. Telescoped porphyry Cu-Mo-Au mineralization, advanced argillic alteration and quartz –sulfide - gold - anhydrite veins in the Thames district, New Zealand. *Mineral. Deposita*. **36**: 623-640 (2001).